Direct X-Ray Observation of a Single Hexagonal Myofilament Lattice in Native Myofibrils of Striated Muscle

Hiroyuki Iwamoto,* Yukihiro Nishikawa,† Jun'ichi Wakayama,* and Tetsuro Fujisawa†
*Life and Environment Division, SPring-8, Japan Synchrotron Radiation Research Institute, Hyogo 679-5198, Japan; and
†Structural Biochemistry Laboratory, RIKEN Harima Institute, SPring-8, Hyogo 679-5148, Japan

ABSTRACT A striated muscle fiber consists of thousands of myofibrils with crystalline hexagonal myofilament lattices. Because the lattices are randomly oriented, the fiber gives rise to an equatorial x-ray diffraction pattern, which is essentially a rotary-averaged "powder diffraction," carrying only information about the distance between the lattice planes. We were able to record an x-ray diffraction pattern from a single myofilament lattice, very likely originating from a single myofibril from the flight muscle of a bumblebee, by orienting the incident x-ray microbeam along the myofibrillar axis (end-on diffraction). The pattern consisted of a number of hexagonally symmetrical diffraction spots whose originating lattice planes were readily identified. This also held true for some of the weak higher order reflections. The spot-like appearance of reflections implies that the lattice order is extremely well maintained for a distance of millimeters, covering up to a thousand of ~2.5-μm-long sarcomeres connected in series. The results open the possibility of applying the x-ray microdiffraction technique to study many other micrometer-sized assemblies of functional biomolecules in the cell.

INTRODUCTION

Cells contain a variety of proteins and enzymes, and they are very often incorporated into large-scale assemblies with very regular structure. A most conspicuous example is striated muscle, in which filamentous polymers of actin and myosin are further integrated into a series of sarcomeres along with other regulatory or accessory proteins. The structure and its function-associated changes have been extensively studied by using the small-angle x-ray diffraction technique, a basically noninvasive method capable of reporting molecular structures in situ with a spatial resolution of an order of nanometers (for reviews, see Hanson, 1968; Wray and Holmes, 1981; Huxley and Faruqi, 1985; Bordas et al., 1991; Popp et al., 1991; Amemiya and Wakabayashi, 1991; Squire and Morris, 1998).

There are many other types of protein assemblies with regular structure in the cell. Some of them are based on cytoskeletal proteins (e.g., microvilli (microfilaments), mitotic spindles (microtubule), eukaryotic flagella, and cilia (microtubules)), while some enzymes polymerize by themselves to form regular structure (e.g., myosin filaments in nonmuscle cells). They are also potential targets for x-ray diffraction studies. However, they have been precluded from x-ray diffraction studies, because their sizes are too small for the conventional x-ray diffraction technique.

The advent of the third-generation synchrotron radiation facilities, featured by insertion devices such as undulators and wigglers, is fundamentally changing this situation. These facilities make it possible to generate high-flux, fine-focused, low-emittance x-ray beams. Even if the beams are sliced to a size of micrometers, the flux is high enough to record diffraction patterns from various materials with a reasonably short time of exposure. The techniques to generate such micrometer- or submicrometer-sized beams range from the use of a glass capillary in combination with pinholes (Riekel et al., 2000) to a multilayer waveguide (Müller et al., 2000). The use of pinholes alone is the least sophisticated, yet suitable for small-angle diffraction recordings as in the present study. With two 2-μm pinholes in series, a beam size of 0.9 μm (full width at one-half maximum) was attained at the specimen position (Fig. 1). By using such small-sized x-ray beams (microdiffraction), high-quality diffraction images have been recorded from collagen fibers, silk threads, wood, and other hard tissues (e.g., Riekel et al., 2000; Busson et al., 1999; Lichtenegger et al., 1999), but the biological applications of the technique have been mainly limited to biopolymers and hard tissues.

The present study was undertaken to see whether the microdiffraction technique can be applied to micrometer-sized protein assemblies, which remain functional in aqueous environment. Specifically, we attempted to record x-ray diffraction pattern from a native (not chemically fixed, dried, or frozen) single myofibril (~2-μm diameter) from striated muscle.

Conventionally, the smallest muscle specimen used for x-ray diffraction studies has been a single skeletal muscle fiber. If a diffraction pattern is to be recorded from a single myofibril, it will be a significant achievement not only because of the specimen size but also in qualitative terms: a single myofibril represents a single lattice of myofilaments (equivalent of a single crystal), whereas the conventional single muscle fiber or a specimen larger than this contains a large number of randomly oriented lattices, and the resulting diffraction pattern is essentially a "powder diffraction" (see Background, Aims, and Strategy for detailed accounts).

Submitted December 3, 2001, and accepted for publication April 3, 2002.
Address reprint requests to Dr. Hiroyuki Iwamoto, Life and Environment Division, SPring-8, Japan Synchrotron Radiation Research Institute, 1-1-1 Kouto, Mikazuki-cho, Sayo-gun, Hyogo 679-5198, Japan. Tel.: 81-791-58-2518; Fax: 81-791-58-0830; E-mail: iwamoto@spring8.or.jp.

0006-3495/02/08/1074/00 $2.00

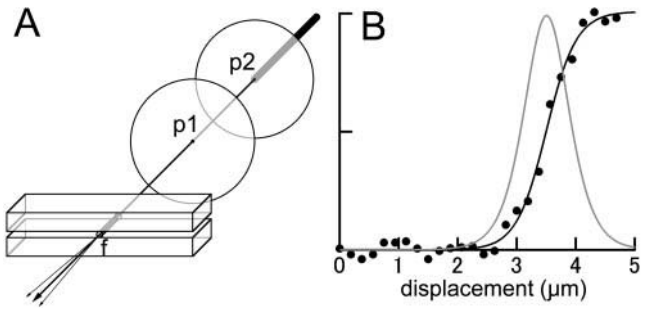

FIGURE 1 Arrangement of the pinhole optics for x-ray microdiffraction and its performance. (*A*) Arrangement. Two pinholes (p1, p2) were placed upstream of the two-axis goniometer sample stage. The sample (*f*) was sandwiched between two 3-mm-wide glass strips. (*B*) Knife-edge scan profile of the beam at the sample position and its derivative. The beam intensity was fitted to a sigmoid before differentiation. The full width at half maximum was 0.9 μm.

Here we report the first diffraction pattern from the single lattice of myofilaments in a native single myofibril from an insect flight muscle by using the microdiffraction technique. The recorded reflections include some of the weak higher order reflections as well as much stronger innermost reflections. This achievement demonstrates the applicability of the x-ray microdiffraction technique to other micrometer-sized protein assemblies as well, thus providing a new means to study the structure and dynamics of this realm of cellular components.

MATERIALS AND METHODS

Materials

A bumblebee, *Bombus* species, was collected in the campus of SPring-8. Its thorax was isolated from the rest of the body and was immersed in the 1:1 mixture of a relaxing solution and glycerol and was stored in a −20°C freezer. On the day of experiment, single fibers (length, ~3 mm) of the longitudinal flight muscle were isolated. The fibers were placed in a rigor solution containing 20 mM butanedione monoxime. A single fiber, either as a whole or after being split to a number of myofibril bundles, was mounted on a 3-mm-wide polylysine-coated glass strip after transferring fiber/fibrils into a rigor solution diluted to one-fourth strength to enhance adhesion to the polylysine coating. The axis of the fiber/myofibrils was made perpendicular to the long axis of the glass strip. The glass strip was covered by another glass strip, and both ends were covered with thin plastic films (Kapton) to avoid evaporation. The whole sample assembly was mounted on the sample stage so that the fiber axis was parallel to the incident x-ray beams (Fig. 1 *A*).

The solutions used for experiments were basically the same as those used for rabbit skinned muscle fibers (Iwamoto, 1995). The undiluted rigor solution had a composition of 120 mM K-propionate, 20 mM imidazole (pH 7.2), 5 mM EDTA, and 5 mM EGTA. The relaxing solution contained 80 mM K-propionate, 20 mM imidazole (pH 7.2), 5 mM $MgCl_2$, 4 mM ATP, and 10 mM EGTA.

X-ray optics

The experiments were conducted at the undulator-based BL45XU beamline of SPring-8 (Fujisawa et al., 2000). The wavelength (λ) of the monochromatized x-ray beams was 0.10 nm. The diffraction images were recorded by a cooled CCD camera in combination with an image intensifier as described (Iwamoto et al., 2001). The specimen-to-detector distance was 2.04 m.

Two pinholes and a sample stage were built into a single assembly. The two pinholes were placed upstream of the two-axis goniometer sample stage. The distance between the two pinholes was 30 mm, and the distance between the sample and the downstream pinhole was 13 mm. The downstream pinhole, functioning as a guard slit, was fixed onto the assembly. The position of the upstream pinhole, as well as that of the sample stage, was adjustable in *x-z* directions with a minimal resolution of ~0.1 μm. The size of the pinhole was either 50 or 2 μm. The 50-μm pinhole was drilled in a 26-μm-thick copper substratum (Sigma Koki, Hidaka, Japan), and the 2-μm pinhole was drilled in a 50-μm-thick tantalum substratum (Lenox Laser, Glen Arm, MD).

To determine the beam size at the sample position, a knife-edge scan was performed and the beam intensity was measured with an ionization chamber placed downstream of the sample stage. The beam intensity, plotted against the knife-edge position, was fitted to a sigmoid and then differentiated to obtain the profile. The full width at one-half maximum was 0.9 μm. The spread of the beam at the detector position was calculated to be comparable with a single pixel of the detector (0.15 mm). Using 2-μm pinholes, patterns of reasonable quality were recorded with an exposure time of 5 s.

Fourier synthesis

The density distribution in the hexagonal myofilament lattice was reconstructed by performing Fourier synthesis by using the integrated intensities of individual diffraction spots. The reflections used for the calculation were 1.0, 1.1, 2.0, 2.2, and 3.1. Each diffraction spot was represented by a single lattice point with an amplitude of the square root of the integrated intensity, and the entire lattice in the reciprocal space was subjected to two-dimensional fast Fourier transform by assuming several combinations of phases. In the presence of hexagonal symmetry, the phase of a reflection can be expressed as either 0°(+) or 180°(−) (Huxley, 1968). For the example in Fig. 4, the assumed phase combination was as reported by Offer et al. (1981) (+,−,+,+,−) (see Fig. 4).

BACKGROUND, AIMS, AND STRATEGY

The equatorial x-ray reflections are the strongest of all the reflections of striated muscle and originate from the hexagonal lattice of myofilaments. These reflections were first recorded from a whole skeletal muscle of frog or rabbit (Huxley, 1953). The relative intensities of these reflections give information about the mass distribution within the unit cell made of actin and myosin, and this distribution changes during contraction or in rigor as a result of actin-myosin interaction (Huxley, 1968; Haselgrove and Huxley, 1973; Squire, 1981). With proper phase information one can in principle reconstruct the mass distribution in the unit cell from these reflections. A sarcomere within a single myofibril constitutes a single hexagonal lattice (equivalent of a single crystal), which generates reflections only when the angle of the incident x-ray beams meet the Bragg conditions. Nevertheless, when one records a single shot of equatorial diffraction pattern from a whole muscle or even a single muscle fiber, all the reflections are recorded at the same time with good reproducibility. This is because a huge number of myofibrils involved allow all the lattice planes to

be sampled with equal statistical probabilities. Therefore, the equatorial diffraction pattern that we usually see in the literature is basically a "powder diffraction" from which all information about the lattice plane orientations is lost. As a result, reflections having similar lattice constants often overlap with each other, and this makes the reconstruction difficult.

It is thus desirable to record x-ray diffraction patterns from a single myofibril containing only a single hexagonal lattice. Besides the experimental difficulty, which would be encountered in recording diffraction from such a minute and fragile specimen, one will have to rotate a single myofibril 360° for all the lattice planes to meet the Bragg conditions. However, there is one way in which all the lattice planes contribute to diffraction at the same time. That is to make the incident x-ray beams parallel to the fiber axis (end-on diffraction). This contrasts to the conventional fiber diffraction technique in which the fiber axis is laid perpendicular to the incident beam. In a rare example, the end-on configuration was used in wood cells and revealed the helical arrangement of the constituent cellulose fibrils (Lichtenegger et al., 1999). However, the end-on configuration has been totally impractical in muscle research, because of the need to clamp both ends and the low energy of x-ray ($\lambda \sim$ 0.15 nm), which has precluded the use of thick specimens.

Our strategy was not to physically isolate single myofibrils but to generate x-ray microbeams (Fig. 1) and shoot at a single myofibril within a single muscle fiber. We preferred insect flight muscle, because its myofibrils, round in cross-section, have relatively little contact with each other due to a high content of mitochondria (Saide and Ullrick, 1973; Squire, 1981; Pringle, 1981; Deatherage et al., 1989), and this makes it ideal for targeting a single myofibril. Insect flight muscle has also an advantage of crystal-quality lattices giving rise to a large number of well-defined reflections (Holmes et al., 1980; Tregear et al., 1990, 1998). Our goal was to observe the hexagonal lattice in reciprocal space, which should also be a hexagonal lattice. The expected positions of the reflections are shown in Fig. 2 *A*. To achieve this, several obstacles had to be overcome. First, to obtain enough reflection intensities, the fiber should be millimeters long, and this meant that each myofibril must be kept very straight and aligned to the x-ray beams very precisely. Second, the myofibril must not be twisted. A 60° twist at one end of a millimeters long myofibril would reduce the pattern to a powder diffraction. Finally, the lattices of all sarcomeres within the myofibril must be strictly in register. Despite all these obstacles, for the first time we were able to observe the single hexagonal lattice in the reciprocal space.

RESULTS

Fig. 2 *B* shows an end-on diffraction pattern from a rigor muscle fiber recorded with 50-μm pinholes (the size of a single fiber). The circular reflections are typical of a "powder diffraction" in which a large number of myofibrils are involved. Besides the strongest 1.0, 1.1 and 2.0 reflections, a number of much weaker higher-order reflections can be seen. No fine structure is seen along the circumference of reflections. With 2-μm pinholes, the patterns look similar to those taken with 50-μm pinholes but fine structure is observed along the circumference of reflections. Not infrequently, the fine structure shows features of a hexagonal lattice: In Fig. 2, *C* and *D*, a bright, well-defined spot appear in every 60° of the 1.0 and 2.0 reflections, and the spots in the two reflections are clearly in phase. Although weaker, a spot is also observed in every 60° of the 1.1 reflection, but this is out of phase with the 1.0 or 2.0 reflection by 30° as expected from the diagram in Fig. 2 *A*. Clearly all these spots originate from a single hexagonal lattice and very likely from a single myofibril. The intensity profiles along the circumference (Fig. 3 *A*) show that ~40% of the total intensity comes from the single lattice, indicating that 40% of the x-ray path in the specimen (1.2 mm) was occupied by a single myofibril.

In the quest for patterns from truly single myofibrils, we split a muscle fiber into a number of myofibrillar bundles. Visual inspections of these bundles showed that the myofibrils at the edge went loose and their density was decreased. Most of the patterns obtained from such bundles were still powder diffraction-like, but we were able to record a few patterns that showed only the hexagonal spots, and the intensities between them were completely missing (Fig. 2, *E* and *F*). The spots in Fig. 2 *E* are well defined, but the absolute intensities are low. Probably only a small part of the x-ray path was occupied by the myofibril and the rest by the buffer. The spots in Fig. 2 *F* are stronger, and even some of the higher order reflections are seen. On close inspection, the higher order reflection spots appear as triplets. The middle of the triplets is stronger than the ones at both ends, and its angular position coincides with that of the 1.1 reflection (Fig. 3 *B*). Therefore, it is identified as the 2.2 reflection. The reflections at both ends appear in the position expected for the 3.1 reflection and are therefore identified as such. In ordinary diffraction patterns these two reflections are closely spaced and difficult to separate, but in the end-on diffraction pattern they appear as isolated spots. Thus, the initial objective for recording from a single myofibril is met.

By taking advantage of these well-separated diffraction spots, we reconstructed the mass distribution in the hexagonal myofilament lattice by Fourier synthesis. The mass distribution shown in Fig. 4 was calculated from the diffraction pattern in Fig. 2 *F* by assuming that the phases of the reflections were (+,−,+,+,−). The densities associated with thick and thin filaments are clearly recognized and are similar to those in the previous report obtained from fiber bundle preparations (Offer et al., 1981). In the reconstruction made by using the intensities of individual diffraction

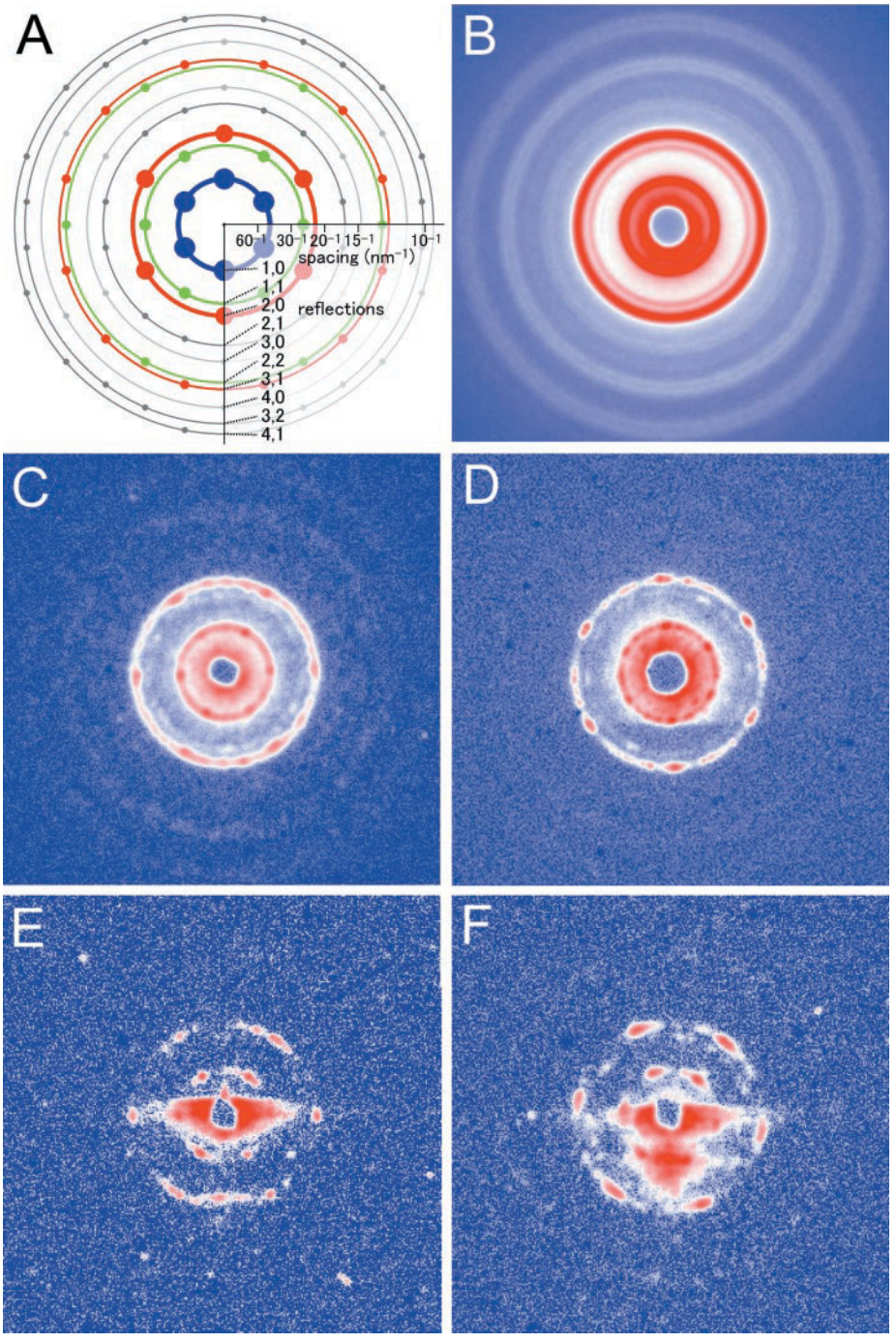

FIGURE 2 End-on diffraction patterns obtained from insect flight muscle. (*A*) Expected positions and approximate intensities (expressed as the size of the spot) of the reflections from a hexagonal lattice. (*B*) End-on diffraction pattern from a muscle fiber in rigor, obtained by using 50-μm pinholes drilled in 26-μm-thick copper. Total exposure time was 6 s (sum of 10 exposures). (*C* and *D*) End-on diffraction patterns from single muscle fibers in rigor, obtained by using 2-μm pinholes drilled in 50-μm-thick tantalum. Total exposure time, 5 s in *C* (single exposure) and 150 s in *D* (sum of 10 exposures). (*E* and *F*) End-on diffraction patterns from single hexagonal lattices, recorded from torn myofibrillar bundles. Exposure time was 5 s. Conditions for recording were the same as in *C* and *D*. The reflection seen below the central beamstop (close to the 2.0 reflection in *E* and close to 1.0 reflection in *F*) is the total reflection from the glass strip, as the myofibril lay close to the glass surface. Note that higher order reflections are seen in *F*.

spots (6 or 12 values for each reflection index, Fig. 4 *A*), the lattice is slightly asymmetrical in that the cross-section of the thick filament is somewhat elongated in vertical direction. On the other hand, in the reconstruction using rotary averaged intensities (corresponding to conventional Fourier syntheses, Fig. 4 *B*), the lattice is perfectly symmetrical.

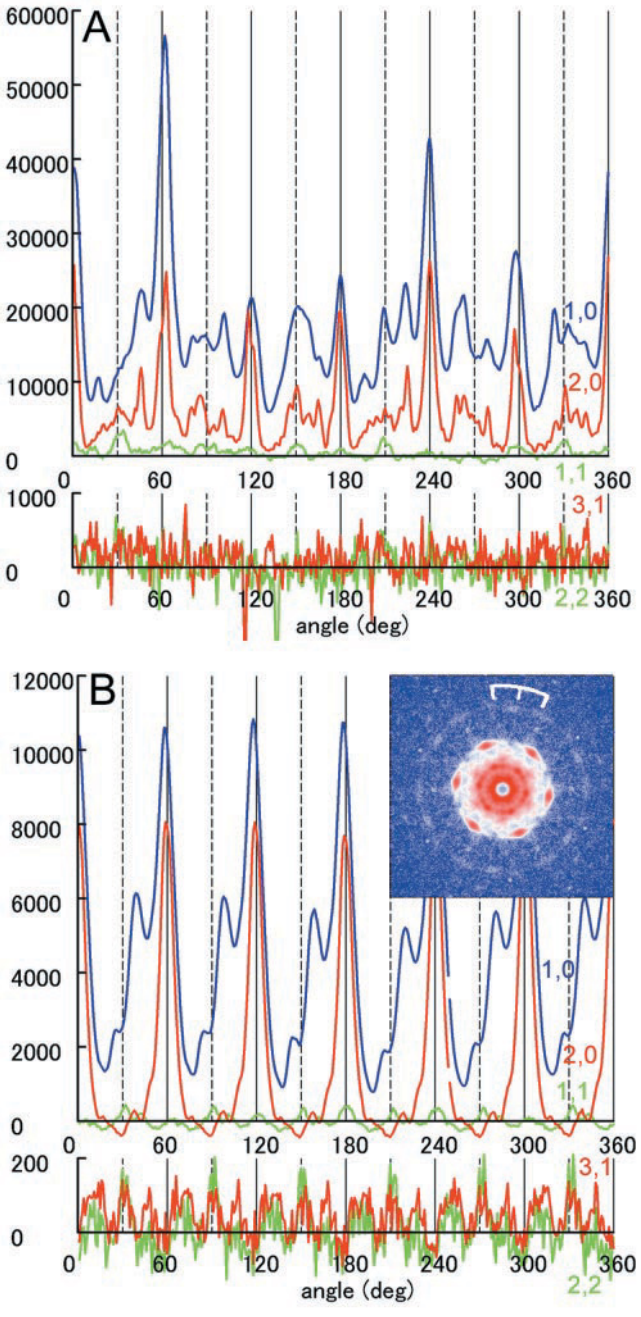

FIGURE 3 Intensity profiles of the reflections plotted along their circumference. (*A*) Profiles from the pattern in Fig. 2 *D*. Vertical lines are the expected position of the reflections (*solid lines*, 1.0, 2.0 reflections, etc.; *broken lines*, 1.1, 2.2 reflections, etc.). Note that the positions of smaller subpeaks have fixed relationship with those of the major peaks. (*B*) Profiles from the pattern in Fig. 2 *F* after 60° rotary averaging (*inset*). In the upper figure, blue, green, and red curves represent the 1.0, 1.1 and 2.0 reflections, respectively. In the lower figure, intensities were measured at the 2.2 (*green*) and 3.1 (*red*) positions, and expressed in 10× magnitude. Intensities were integrated in the range of ±3 pixels along the radius. Therefore, the ranges of integration for the 2.2 and 3.1 reflections overlap with each other. The subpeaks of the 1. reflection in (*B*) are artifacts due to the total reflection from the glass. The peaks of the 1.1 reflection on the solid lines are due to the slope of the 2.0 reflection. One count in the ordinate corresponds to one bit of the 14-bit resolution A-D converter output of the CCD camera. Note that in *B*, the outer reflections (identified as 3.1 and 2.2 reflections) appear in triplets of isolated spots (*white bracket* in the *inset*).

DISCUSSION

In the present paper we were able to record the first x-ray diffraction pattern from a single hexagonal lattice of native myofilaments of striated muscle. Although the isolated diffraction spots were not obtained from isolated single myofibrils, we believe that they came from single myofibrils. This is because 1) patterns suggestive of a hexagonal lattice were observed for the first time when we reduced the beam size to less than the diameter of a single myofibril, and 2) the myofibrils in flight muscles are only loosely connected to each other and it is unlikely that the lattices in neighboring myofibrils are exactly in register.

The significance of this achievement is summarized in four points. 1) The diffraction patterns were obtained from a native specimen, which is ~1000 times smaller than the conventionally used smallest muscle specimen (single muscle fiber) with an exposure time of as short as five seconds. 2) This is the recording from a single hexagonal lattice (equivalent of a single crystal) as opposed to the conventional "powder diffraction." 3) This represents the application of a novel technique of "end-on diffraction" to muscle specimen. 4) The lattice structure was resolved from a very thick (millimeters) specimen. Discussion for each point follows.

Diffraction recorded from micrometer-sized native specimen

The present results demonstrate that, by using x-rays from the third-generation synchrotron radiation sources, good diffraction patterns can be obtained from micrometer-sized native, hydrated protein assembly with a practical time of exposure. This means that the technique used here may be applied to other micrometer-sized protein assemblies in the cell as listed earlier, as well as some of the muscle specimens in which contractile apparatus has developed to a much lesser extent (e.g., cultured myocytes).

It should also be noted that the recordings were made without using a focusing optics (except for the standard bent mirrors in the optics hutch). A focusing optics would increase the total flux on the specimen at the expense of small-angle resolution. With the nonfocusing optics as used here, the 1.0 reflection from the hexagonal lattice with a unit cell size of ~45 nm was readily resolved.

Diffraction from a single hexagonal lattice

From single hexagonal lattices we were able to record diffraction patterns in which each reflection appeared as a separate spot despite the relatively short camera length (~2

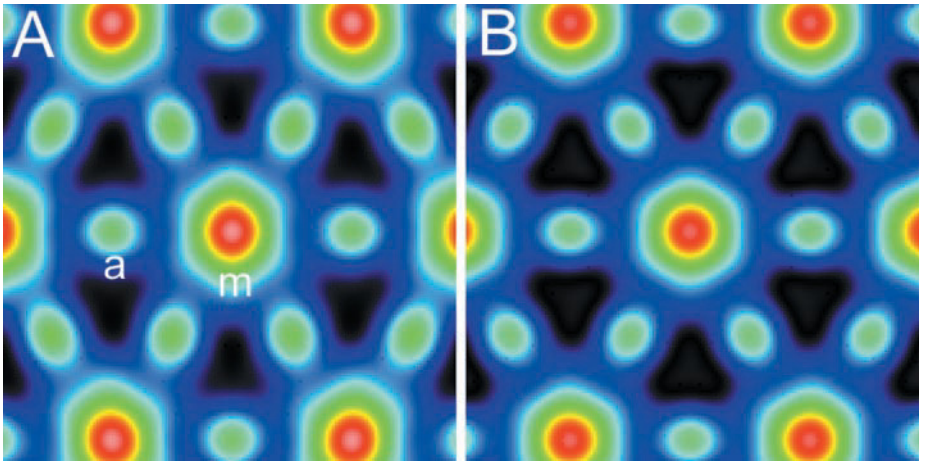

FIGURE 4 Example of the electron densities of the hexagonal myofilament lattice reconstituted by the direct two-dimensional Fourier synthesis from the diffraction pattern from a single hexagonal lattice in Fig. 2 *F*. (*A*) Reconstruction made by using the intensities of individual diffraction spots; (*B*) reconstruction using rotary averaged intensities. a, Actin filament densities; m, myosin filament densities. The phases of the reflections (1.0, 1.1, 2.0, 2.2, and 3.1) were assumed to be (+,−,+,+,−) (Offer et al., 1981). Densities increase in the order of black-blue-green-yellow-red-white.

m). In the case of conventional equatorial reflections, closely spaced two reflections (such as 2.2 and 3.1) are often difficult to separate unless a long camera length (~5 m) is used. The diffraction from a single lattice has also a merit that the reconstruction can be made by using the intensities of individual reflection spots as was done here (Fig. 4 *A*), as opposed to the conventional reconstruction, which uses a single summed value of intensities for each lattice index. This feature would be useful in the case of hexagonally asymmetrical lattice (e.g., the cross-section of a thick filament has a specific orientation with respect to the lattice (Huxley and Brown, 1967; Luther and Squire, 1980)). In this case, reflections such as 3.1 and 1.3 may not be equivalent. Reconstruction of asymmetrical lattice would be possible only from the diffraction from a single lattice.

In the present results, a slight asymmetry was observed in the reconstituted lattice (Fig. 4 *A*). This asymmetry originates from the lower order reflections. One must be careful about its interpretation because a slight tilt of the specimen with respect to the beampath could result in a similar effect.

End-on diffraction

The end-on diffraction technique enabled us to record all the reflections from a single myofibril in a single shot without the necessity to rotate it 360° or to isolate it from a muscle fiber. The end-on diffraction was again made easier by the third-generation synchrotron facility, which allows the use of short wavelength ($\lambda = 0.10$ nm as opposed to conventional $\lambda \sim 0.15$ nm) for which optimum specimen thickness is ~3.4 mm as opposed to ~1 mm. However, with a focusing optics and/or a beamline with higher flux (e.g., BL40XU at SPring-8, Inoue et al., 2001), high-quality end-on diffraction would be recorded from thinner specimens. This would be especially advantageous for specimens other than muscle contractile apparatus.

Unlike the conventional equatorial reflections, end-on diffraction like that recorded here does not represent the Bragg case. It is rather a modified case of diffraction from a two-dimensional lattice (a stack of planar gratings, each having a finite thickness). A simple theoretical treatment of such diffracting objects are given in the Appendix. As is argued there, it is likely that these planar hexagonal lattices (i.e., sarcomeres) diffract x-rays independently without interference between two adjacent planes.

Lattice structure resolved from thick specimen

At a first glance, the end-on diffraction patterns as shown in Fig. 2, *E* and *F* resemble a laser diffraction pattern or a direct Fourier transform of an electron micrograph of a thin cross-section (e.g., Huxley, 1968; Yu et al., 1977; Luther and Squire, 1980). The fundamental difference is that the thickness of the specimen is only ~100 nm in the case of electron micrograph (representing only a small fraction of the sarcomere length), whereas it is millimeters in the case of the present end-on diffraction patterns (hundreds to a thousand of sarcomere lengths). This means that the lattice register of the thick specimen is as good as in the thin section.

The *z* line, which connects two adjacent sarcomeres, is constructed in such a way that, in principle, no twist is generated between the two adjacent lattices. At the same time, however, it has been reported that the *z* line is constructed to position a thick filament at the trigonal point of the three thin filaments in the opposite sarcomere (Ashhurst, 1967, 1971; Saide and Ullrick, 1973; Deatherage et al., 1989). This arrangement produces a systematic stagger between the adjacent lattices as shown in Fig. 5, *A*. A consequence of this stagger on the x-ray diffraction pattern would be a marked enhancement of the 1.1 and 2.2 reflections. (As discussed in Appendix, the filaments in the adjacent sarcomeres are close enough to cause interference if they are perfectly aligned with respect to each other.) However, such enhancement has not been observed in either conventional or end-on diffraction patterns. A possible cause for the

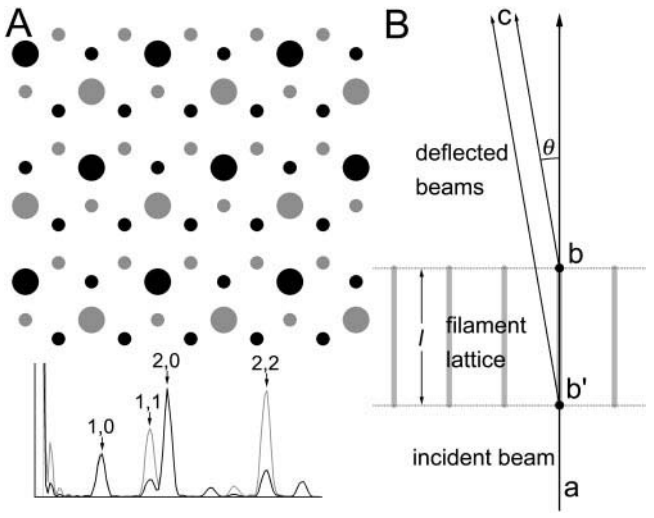

FIGURE 5 Schematized lattices of insect flight muscle sarcomeres. (*A*) Above, the systematic stagger of myofilaments between the two adjacent sarcomeres (Ashhurst, 1967; Saide and Ullrick, 1973; Deatherage et al., 1989). The filament on one side of the *z* line are in black, and those on the other side are in gray. Below, the rotary-averaged Fourier transform of the lattices shown above. (*Black curve*) Transform of either of the two lattices; (*gray curve*) transform of the two lattices superposed. Note the enhancement of the 1.1 and 2.2 reflections in the curve for the superposed lattices. (*B*) Diagram showing the principle of end-on diffraction from a myofilament lattice.

absence of interference is again the flexible *z*-line structure, as discussed in Appendix. A similar situation is also found in vertebrate skeletal muscle in which a thin filament in a sarcomere originates from the *z* line at a position half way between the two thin filaments in the opposite sarcomere (see Squire, 1981). Such an arrangement should result in negative interference. Nevertheless, a reflection indexed to the tetragonal lattice of the *z* line and adjacent parts of the thin filaments has long been observed (Elliott et al., 1967; Yu et al., 1977; Irving and Millman, 1992).

The arguments we have made so far point to two notions that may sound contradictory at first, i.e., 1) flexible connections between the adjacent sarcomeres, which keeps the adjacent lattices out of register, possibly by displacing the lattices laterally, and 2) the long range register of lattices in a sense that little twist is involved. The coexistence of the short-range disorder and the long-range register is not impossible, because it would be easier to produce a lateral displacement between adjacent lattices than to produce a twist. A lateral displacement may be made with a small distortion in each component of the *z* line, whereas a twist requires an increasing amount of distortion with an increasing radius across the myofibril.

Even with this resistance to a twist, the observed extent of the long-range register is still surprising if one considers the softness of the unfixed threadlike hydrated protein assemblies and every distorting force they would experience in the process of preparation. The reflections appearing as spots (at least up to the 3.1 reflection) mean that this register extends to hundreds or a thousand of sarcomeres. Because the length of the specimen is almost equal to the whole length of muscle fibers, it is quite possible that the register is preserved along the entire length of a myofibril in situ. Then one may say that a myofibril is a single crystal grown in the body of an insect, and it is a crystal that functions.

CONCLUSION

The present study revealed that a large-scale protein assembly can be built in a cell with an unprecedented extent of order. The combination of the technologies used here (x-ray microdiffraction applied to native proteins, end-on diffraction, etc.) along with the use of the third-generation, undulator-based synchrotron x-ray sources expands the spectrum of the structural studies of muscle. At the same time, the same technologies make the possibility realistic that structure of other micrometer-sized protein assemblies can be analyzed by x-ray diffraction in situ.

APPENDIX

Here a simple theoretical consideration about end-on diffraction is given. Consider a planar hexagonal lattice made of diffracting points in an aqueous environment (Fig. 5 *B*), each of which having a finite depth (l). When l is of the order of micrometers and the diffracting object has a density not very different from that of water, the absorption of x-ray along the object is negligible at a wavelength $\lambda = 0.1$ nm, so that the object scatters x-rays uniformly along its length. At a deflection angle θ, the path lengths (a-b-c and a-b′-c) are different for the beams deflected at both ends of the object and therefore they have different phases. The phase difference $\Delta\phi$ is expressed as

$$\Delta\phi = 2\pi l(1/\cos\theta - 1)/\lambda,$$

and the structure factor of the object $F(\theta)$ is obtained by integrating the quantity $\rho \times \exp(i\phi)$ over the entire length of the object, in which ρ is the density.

If l is small enough, $\Delta\phi$ is negligible, and the $F(\theta)$ increases in proportion to l. With greater l, however, the beams start to interfere negatively and the $F(\theta)$ approaches 0 as $\Delta\phi$ approaches π. For the 1.0 reflection, the value of $(1/\cos\theta - 1)$ is $\sim 1/500$, and the value of l at which $\Delta\phi = \pi$ is calculated to be ~ 25 μm. This is much greater than the length of the myofilaments. Therefore, the phase difference effect is negligible within a single sarcomere, and the beams scattered by a myofilament should contribute productively to the reflection intensities. However, the phase difference effect may be more pronounced in higher order reflections.

The above consideration may be extended to sarcomeres connected in series. If the adjacent sarcomeres are perfectly aligned to each other and the beams are perfectly coherent, it is expected that the beams scattered from all the sarcomeres will interfere with each other in a manner stated above, and the integrated reflection intensities will never be proportional to the number of sarcomeres in series. On the contrary, the fact is that quite strong reflections have been recorded. Therefore, the explanation for this observation should be either 1) the sarcomeres in a single myofibril are not perfectly aligned (they are connected to each other by flexible links within the *z* lines, or the sarcomeres themselves are flexible to some extent), or 2) the x-rays have only a short coherence length along the beampath or both. Concerning the latter, the Wiener-Khintchine theorem predicts that the

coherence length of beams is approximated as $\lambda^2/\Delta\lambda$ (e.g., Kikuta, 1992). In the beamline BL45XU in SPring-8, the energy resolution $\Delta\lambda/\lambda$ is $\sim 10^{-4}$. Therefore, the coherence length should be ~ 1 μm. This value is much shorter than the aforementioned diffraction limit of 25 μm and precludes the long-range interference. However, this is still long enough to allow intersarcomere interference across the *z* line. This interference would cause an enhancement of specific reflections, but no such enhancement was observed (see Discussion). The lack of enhancement supports the idea that the *z* line provides a flexible linkage between two adjacent sarcomeres. Taken together, it would be appropriate to regard an entire myofibril as a stack of independently diffracting planar two-dimensional gratings so that the reflection intensities are proportional to the number of gratings or sarcomeres.

We thank Dr. N. Yagi for his helpful comments and Ms. R. Ryu for her technical assistance. This work was performed under approval of the SPring-8 Proposal Review Committee (proposal Nos. 1999A0098-NL-np, 1999B0144-CL-np, 2000A0170-NL-np, 2000B0128-NL-np, and 2001A0121-NL-np). Supported by SPring-8 Joint Research Promotion Scheme of Japan Science and Technology Corporation.

REFERENCES

Amemiya, Y., and K. Wakabayashi. 1991. Imaging plate and its application to X-ray diffraction of muscle. *Adv. Biophys.* 27:115–128.

Ashhurst, D. E. 1967. Z-line of the flight muscle of Belostomatid water bugs. *J. Mol. Biol.* 27:385–389.

Ashhurst, D. E. 1971. The Z-line in insect flight muscle. *J. Mol. Biol.* 55:283–285.

Bordas, J., G. P. Diakun, J. E. Harries, R. A. Lewis, G. R. Mant, M. L. Martin-Fernandez, and E. Towns-Andrews. 1991. Two-dimensional time resolved X-ray diffraction of muscle: recent results. *Adv. Biophys.* 27:15–33.

Busson, B., P. Engström, and J. Doucet. 1999. Existence of various structural zones in keratinous tissues revealed by X-ray microdiffraction. *J. Synchrotron Rad.* 6:1021–1030.

Deatherage, J. F., N. Cheng, and B. Bullard. 1989. Arrangement of filaments and cross-links in the bee flight muscle Z-disk by image analysis of oblique sections. *J. Cell Biol.* 108:1775–1782.

Elliott, G. F., J. Lowy, and B. M. Millman. 1967. Low-angle X-ray diffraction studies of living striated muscle during contraction. *J. Mol. Biol.* 25:31–45.

Fujisawa, T., K. Inoue, T. Oka, H. Iwamoto, T. Uruga, T. Kumasaka, Y. Inoko, N. Yagi, M. Yamamoto, and T. Ueki. 2000. Small-angle X-ray scattering station at the SPring-8 RIKEN beamline. *J. Appl. Cryst.* 33:797–800.

Hanson, J. 1968. Recent x-ray diffraction studies of muscle. *Q. Rev. Biophys.* 1:177–216.

Haselgrove, J. C., and H. E. Huxley. 1973. X-ray evidence for radial cross-bridge movement and for the sliding filament model in actively contracting skeletal muscle. *J. Mol. Biol.* 77:549–568.

Holmes, K. C., R. T. Tregear, and J. Barrington-Leigh. 1980. Interpretation of the low angle X-ray diffraction from insect flight muscle in rigor. *Proc. R. Soc. Lond. B.* 207:13–33.

Huxley, H. E. 1953. X-ray analysis and the problem of muscle. *Proc. R. Soc. B.* 141:59–62.

Huxley, H. E. 1968. Structural difference between resting and rigor muscle: evidence from intensity changes in the low-angle equatorial X-ray diagram. *J. Mol. Biol.* 37:507–520.

Huxley, H. E., and W. Brown. 1967. The low-angle X-ray diagram of vertebrate striated muscle and its behaviour during contraction and rigor. *J. Mol. Biol.* 30:383–434.

Huxley, H. E., and A. R. Faruqi. 1985. Time-resolved X-ray diffraction studies on vertebrate striated muscle. *Ann. Rev. Biophys. Bioeng.* 12: 381–417.

Inoue, K., T. Oka, T. Suzuki, N. Yagi, K. Takeshita, S. Goto, S., and T. Ishikawa. 2001. Present status of high flux beamline (BL40XU) at SPring-8. *Nucl. Instr. Methods Phys. Res. A.* 467/468:674–677.

Irving, T. C., and B. M. Millman. 1992. Z-line/I-band and A-band lattices of intact frog sartorius muscle at altered interfilament spacing. *J. Muscle Res. Cell Motil.* 13:100–105.

Iwamoto, H. 1995. Evidence for increased low force cross-bridge population in shortening skinned skeletal muscle fibers: implications for actomyosin kinetics. *Biophys. J.* 69:1022–1035.

Iwamoto, H., K. Oiwa, T. Suzuki, and T. Fujisawa. 2001. X-ray diffraction evidence for the lack of stereospecific protein interactions in highly activated actomyosin complex. *J. Mol. Biol.* 305:863–874.

Kikuta, S. 1992. X-Ray Diffraction and Scattering, Vol. 1 (in Japanese). University of Tokyo Press, Tokyo.

Lichtenegger, H., M. Müller, O. Paris, C. Riekel, and P. Fratzl. 1999. Imaging of the helical arrangement of cellulose fibrils in wood by synchrotron X-ray microdiffraction. *J. Appl. Cryst.* 32:1127–1133.

Luther, P. K., and J. M. Squire. 1980. Three-dimensional structure of the vertebrate muscle A-band: II. The myosin filament superlattice. *J. Mol. Biol.* 141:409–439.

Müller, M., M. Burghammer, D. Flot, C. Riekel, C. Morawe, B. Murphy, and A. Cedola. 2000. Microcrystallography with an X-ray waveguide. *J. Appl. Cryst.* 33:1231–1240.

Offer, G., J. Couch, E. O'Brien, and A. Elliott. 1981. Arrangement of cross-bridges in insect flight muscle in rigor. *J. Mol. Biol.* 151:663–702.

Popp, D., Y. Maeda, A. A. E. Stewart, and K. C. Holmes. 1991. X-ray diffraction studies on muscle regulation. *Adv. Biophys.* 27:89–103.

Pringle, J. W. S. 1981. The Bidder lecture, 1980: the evolution of fibrillar muscle in insects. *J. Exp. Biol.* 94:1–14.

Riekel, C., M. Burghammer, and M. J. Müller. 2000. Microbeam small-angle scattering experiments and their combination with microdiffraction. *J. Appl. Cryst.* 33:421–423.

Saide, J. D., and W. C. Ullrick. 1973. Fine structure of the honeybee Z-disc. *J. Mol. Biol.* 79:329–337.

Squire, J. M. 1981. The Structural Basis of Muscular Contraction. Plenum Press, New York.

Squire, J. M., and E. P. Morris. 1998:A new look at thin filament regulation in vertebrate skeletal muscle. *FASEB J.* 12:761–771.

Tregear, R. T., R. J. Edwards, T. C. Irving, K. J. V. Poole, M. C. Reedy, H. Schmitz, E. Towns-Andrews, and M. K. Reedy. 1998. X-ray diffraction indicates that active cross-bridges bind to actin target zones in insect flight muscle. *Biophys. J.* 74:1439–1451.

Tregear, R. T., K. Wakabayashi, H. Tanaka, H. Iwamoto, M. C. Reedy, M. K. Reedy, H. Sugi, and Y. Amemiya. 1990. X-ray diffraction and electron microscopy from Lethocerus flight muscle partially relaxed by adenylylimidodiphosphate and ethylene glycol. *J. Mol. Biol.* 214: 129–141.

Yu, L. C., R. W. Lymn, and R. J. Podolsky. 1977. Characterization of a non-indexible equatorial X-ray reflection from frog sartorius muscle. *J. Mol. Biol.* 115:445–464.

Wray, J. S., and K. C. Holmes. 1981. X-ray diffraction studies of muscle. *Ann. Rev. Physiol.* 43:553–565.